Journal of the European Ceramic Society 19 (1999) 1615–1622

PII: S0955-2219(98)00264-7
0955-2219/99/$ - see front matter

DLVO Theory and Clay Aggregate Architectures Formed with $AlCl_3$

A. C. Pierre* and K. Ma

Department of Mining, Metallurgical and Petroleum Engineering, The University of Alberta, Edmonton, AB, Canada T6G 2G6

(Received 17 September 1998; accepted 26 October 1998)

Abstract

To understand the conditions in which clay aggregates with a different architecture can be formed, sedimentation experiments were undertaken of kaolinite and montmorillonite suspensions mixed with Al electrolyte. The aggregates' architecture was observed in a scanning electron microscope after supercritical drying with liquid CO_2 and relatively acceptable correlation with the value of the zeta potential of the clay particles was obtained. Hence, in a first approximation, it appears that the texture of clay aggregate is driven by electrostatic interactions between particles, as expressed in the Derjaguin, Landau, Verwey and Overbeek (DLVO) theory. The main aggregate architectures which were observed included sediments with a relatively uniform porosity formed by accumulation of particles under gravity, such as without any Al electrolyte, and flocs with an architecture qualitatively consistent with diffusion limited aggregates (DLA), when Al electrolyte were added to the suspension. © *1999 Published by Elsevier Science Limited. All rights reserved*

Keywords: DLVO theory, suspensions, electron microscopy, clays, traditional ceramics.

1 Introduction

Clays are important engineering materials, and although they do not belong to the class of advanced ceramics, their study can bring valuable information for the processing of all ceramics made by sintering of platelike particles. In particular, it is well known that sintering can be significantly affected by aggregate architecture as resulting from green material processing, which in turn is driven by liquid medium conditions. Hence, it is important to understand the conditions in which different types of aggregates can form. Although many studies have addressed the texture of clay aggregates, the present paper also addresses this task in a simple limited set of conditions, after a treatment according to which clay particles are known to carry electric charges with same sign on both their edges and their faces. The aim actually was to establish a simple correlation between the texture of aggregates observed in a scanning electron microscope after supercritical drying in CO_2, as well as the sedimentation kinetics on one hand, and the value of the particles zeta potential on the other hand.

2 Experimental Procedure

The kaolinite investigated was 'Hydrite UF' from the Georgia Kaolin Company. This kaolinite was first treated with sodium phosphate according to a standard procedure to convert it to the sodium form.[1] Next, suspensions containing 0·5% (by mass) kaolinite were prepared in 100 ml graduated cylinders with an inside diameter of 28 mm. A height of 1 cm in a cylinder corresponded to a volume of 6·16 ml. Dispersion of the clay was achieved with 1 ml of 0·5 M $Na_4P_2O_7$ for 100 ml of total suspension volume, a procedure which is known to provide negative charges both to the faces and edges of the kaolinite particles.[2]

The Al electrolyte used was $AlCl_3$. For some series of samples, termed suspensions mixed with unaged $AlCl_3$, this electrolyte was dissolved in distilled water at room temperature just before mixing with clay suspensions. For other series of samples, termed suspensions mixed with aged $AlCl_3$, beakers containing 500 ml of a 0·5 M $AlCl_3$ solution in

*To whom correspondence should be addressed at Université Claude Bernard-Lyon 1, Institut de Recherches sur la Catalyse, 2 Avenue Albert Einstein, 69626 Villeurbanne cedex, France.

distilled water were prepared, and they were allowed to age for a month before mixing in tile clay suspension. No obvious precipitation occurred during this ageing process.

The pH which were studied with unaged $AlCl_3$ were 2, 4, 6, 8, 9·5 and 12 and these values were achieved by addition of HCl or NaOH. The concentrations of unaged $AlCl_3$ which were investigated were 1, 2, 5, 10, and 50 mM, respectively, for each pH. Similar studies were made with aged $AlCl_3$ at concentrations of 1, 2, 5, 10, and 50 mM and at pH 2, 4, 6, 9.5 and 12.

The montmorillonite investigated was 'Na-SWy' from the Clay repository at the University of Missouri. As with kaolinite, the sedimentation of montmorillonite in the presence of unaged or of aged $AlCl_3$ was studied. Each cylinder contained 100 ml of a suspension with 1% Na montmorillonite (by mass). Before adding any electrolyte, the suspension pH was $\approx 9{\cdot}5$. The pH values investigated in the present study were 2, 4, 6, 9.5 and 12 and they were realized by adding HCl or NaOH to the suspensions, depending on the pH. The concentrations of unaged as well as aged $AlCl_3$ were 0·17, 0·33, 1, 2, 3·3, 5, 10, and 20 mM at each pH.

The zeta potential (ζ) of clay particles in some suspensions was determined in a microelectrophoresis Mark II apparatus from the Rank Brothers company. The measurements were performed for one set of stationary conditions inside the cell. The electrophoretic mobility of a minimum of five particles were successively measured, first when applying the electric field in one direction, then after reversing the polarity of the applied electric field. The average value was recorded. Because 0·5% (by mass) kaolinite and 1% (by mass) montmorillonite suspensions were too dense to directly, measure their zeta potential, these clay suspensions were first diluted to 0·05% and to 0·01%, respectively, in distilled water. In each case, and just before measuring the zeta potential, the pH was adjusted to the value the suspension had before dilution, by addition of HCI or NaOH, depending on the required pH. In the same way, some Al electrolyte was added to each clay suspension so as to maintain the initial concentration of these electrolytes before dilution.

Zeta potential data were obtained for kaolinite-unaged $AlCl_3$ suspensions at the pH values 2, 4, 6, 9·5, and 12, and unaged $AlCl_3$ concentrations of 0, 1, 2, 5, and 10 mM. Other data were measured on montmorillonite-unaged $AlCl_3$ suspensions at the pH values of 2, 4, 6, 9.5 and 11, and unaged $AlCl_3$ concentrations of 0·5, 1, 3·5, and 10 mM.

Finally, clay sediment samples were dried by the CO_2 supercritical drying method as described previous publications[3,4] and they were examined in a Hitachi S-2700 SEM equipped with a LINK-EXL. These observations were mostly done at 10 kV.

3 Experimental Results

The sedimentation behavior of Na-kaolinite and Na-Montmorillonite suspensions mixed with unaged or aged Al electrolyte were very similar to the sedimentation behavior previously reported for Fe electrolyte.[3,4] Three types of sedimentation were observed: flocculation, accumulation or mixed accumulation–flocculation. Their characteristics are illustrated in Fig. 1. In flocculation sedimentation, a suspension separated very fast into a sediment and a clear supernatant liquid on top of the sediment. The sediment was relatively thick and it had uniform visual characteristics. The separation interface between the sediment and the supernatant liquid was sharp and it moved downwards with time. That is to say the flocculated sediment underwent a compacting process. Typical kinetics data for this type of sedimentation are reported in Fig. 2(a).

In accumulation sedimentation, independent particles or aggregates had the time to fall downwards and to accumulate at the bottom of a cylinder, before they could aggregate to each other to build a single uniform floc. A sharp interface separated the accumulated sediment from the remaining clay suspension. This sharp interface moved upwards with time, as more particles accumulated. The remaining suspension, on top of the accumulated sediment did not have a uniform visual characteristics. Instead, the particles density decreased gradually with increasing height in the cylinder, so that no sharp interface separated the remaining suspension from the supernatant liquid. Typical

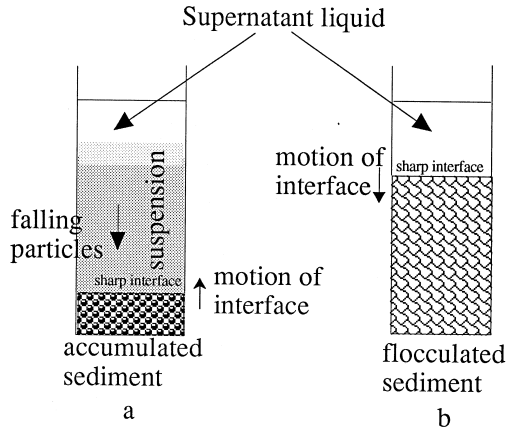

Fig. 1. Sedimentation behavior modes of kaolinite and montmorillonite suspensions mixed with $AlCl_3$ electrolyte: (a) accumulation sedimentation; (b) flocculation sedimentation.

kinetics data for this type of sedimentation are reported in Fig. 2(b).

Mixed flocculation–accumulation sedimentation was also observed. In this case, some particles could accumulate at the bottom of a cylinder at the beginning of a sedimentation process. During this stage, the upwards displacement of a sharp interface between the accumulated sediment and the remaining suspension was observed. However, after some time the remaining suspension could form a flocculated sediment with a uniform visual characteristics, on top of the accumulated sediment. After an intermediate transition period when no sharp interface could be observed, the downwards displacement of the sharp interface between the flocculated sediment and the remaining clear suspension could finally be recorded. Typical mixed sedimentation kinetics are reported in Fig. 3. In this case, the accumulated sediment was very thin. Most of the sediment thickness was of the flocculated type, on top of the accumulated sediment.

Diagrams which summarize the sedimentation behavior of Na-HUF kaolinite suspensions mixed with unaged $AlCl_3$, are reported in Fig. 4(a). No significant difference was found between aged and unaged $AlCl_3$. Similarly, diagrams for the sedimentation behavior of 1% Na-montmorillonite suspensions mixed with unaged $AlCl_3$ are reported in Fig. 5(a). The field of conditions where accumulation sedimentation occurred was slightly more extended with aged than with unaged $AlCl_3$.

In the cases where flocculation occurred, the measured initial settling rates are reported in Figs 6 and 7 for kaolinite and montmorillonite

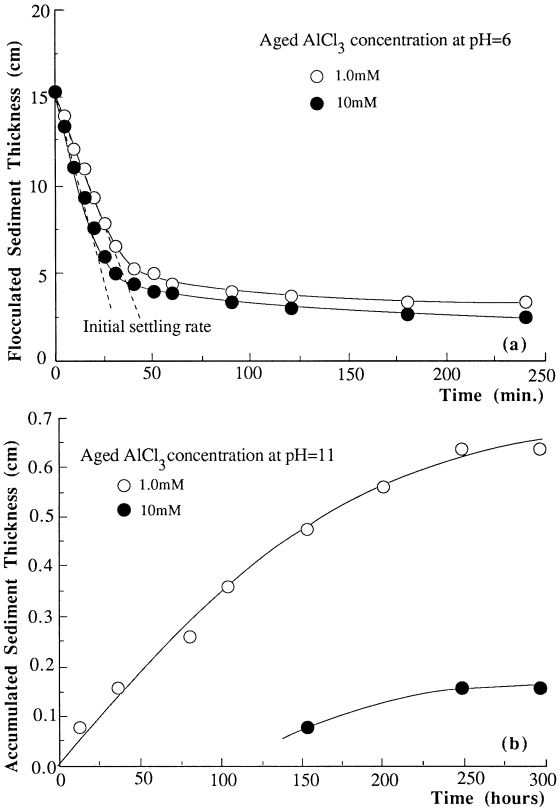

Fig. 2. Displacement kinetics of sharp interfaces in 0·5% (by mass) Na-kaolinite suspensions: (a) flocculated sediment–supernatant liquid interface with aged $AlCl_3$ concentrations of 1 and 10 mM at pH = 6; (b) accumulated sediment–diffuse suspension interface with aged $AlCl_3$ concentrations of 1 and 10 mM at pH = 11.

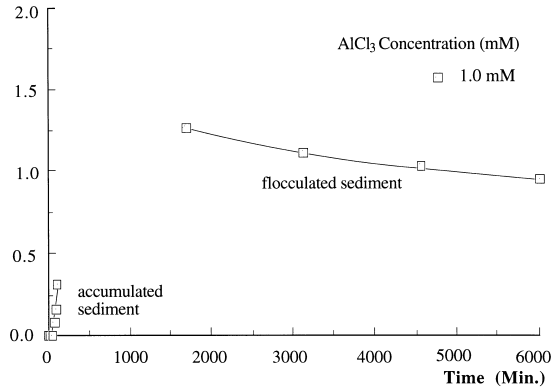

Fig. 3. Sedimentation kinetics of 0·5% Na-HUF Kaolinite suspensions with an unaged $AlCl_3$ concentration of 1 mM at pH = 6.

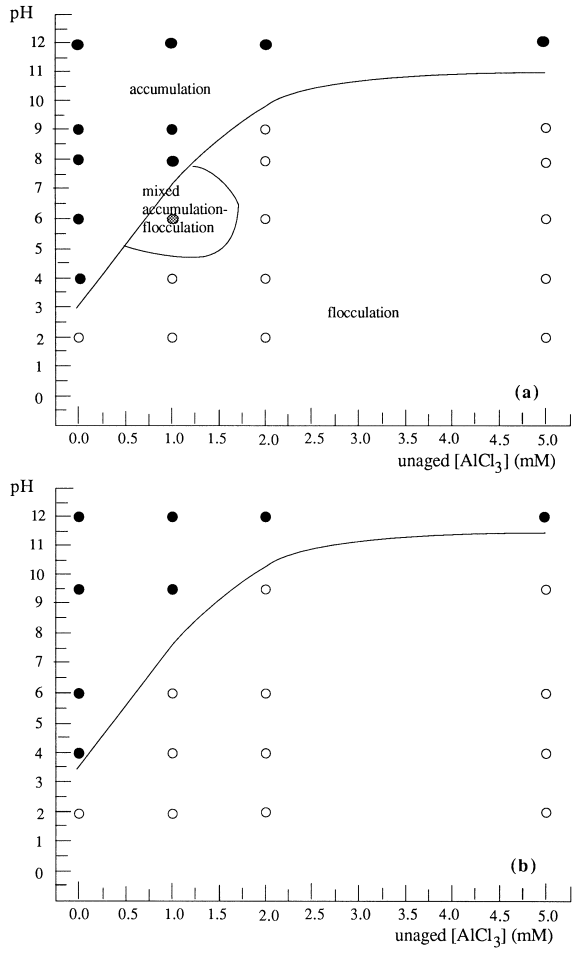

Fig. 4. Compared sedimentation diagrams of 0·5% Na-kaolinite suspensions mixed with unaged $AlCl_3$: (a) experimental observations. The solid, open and semi-open dots respectively indicate accumulation, flocculation and mixed behavior; (b) diagram from the zeta potential data. The solid and open dots respectively indicate zeta potential absolute values $|\zeta| \geq 12$ mV and $|\zeta| \leq 12$ mV.

respectively. This initial settling rate was at least 100 times faster for kaolinite than for montmorillonite. For kaolinite, no significant difference could be noticed between aged and unaged $AlCl_3$. On the other hand, in the case of montmorillonite, a significant difference could be noticed between aged and unaged $AlCl_3$.

The final sediment thicknesses are reported in Figs 8 and 9 for kaolinite and montmorillonite respectively. This final sediment volume was of the order of 5 times higher for montmorillonite than for kaolinite. In the case of kaolinite, as for the initial settling rate, no significant difference was noted between aged and unaged $AlCl_3$. On the other hand, a significant difference between aged and unaged $AlCl_3$ was observed for montmorillonite. Aged $AlCl_3$ at a concentration > 2 mM had a tendency to decrease the final sediment volume, while below this concentration it increased this volume.

The data on zeta potential of kaolinite particles mixed with unaged $AlCl_3$ are reported in Fig. 10. At pH$\leq$9·5, the addition of unaged $AlCl_3$ at a concentration from 1 to 9 mM, increased the zeta potential from a negative to a slightly positive value, independent of pH and $AlCl_3$ concentration. In the case of montmorillonite particles in suspensions mixed with unaged $AlCl_3$, the zeta potential changed from a negative to a positive value at all pH, as soon as a small concentration of $AlCl_3$ was added (Fig. 11).

These data on kaolinite zeta potential could be used to build sedimentation diagrams. For instance in Fig. 4(b), the data could be divided in two fields as a function of the absolute value of the zeta potential $|\zeta|$. One field with open dots was for $|\zeta| \leq 12$ mV. The other field with solid dots was for $|\zeta| \geq 12$ mV. The diagram which was obtained was very similar to the actual sedimentation diagram in Fig. 4(a). Such a coincidence indicates that accumulation occurred when ζ had a high absolute magnitude ($\geq$12 mV), and flocculation when ζ had a low absolute magnitude ($\leq$12 mV), which means that sedimentation kinetics as well as aggregates texture were controlled by electrostatic interactions. A similar comparison could be established for mixed montmorillonite unaged $AlCl_3$ suspensions. However, a good fit between the actual sedimentation diagram [Fig. 5(a)] and a diagram from the zeta potential [Fig. 5(b)] required to chose $|\zeta| = 2$ mV as the critical value between accumulation and flocculation.

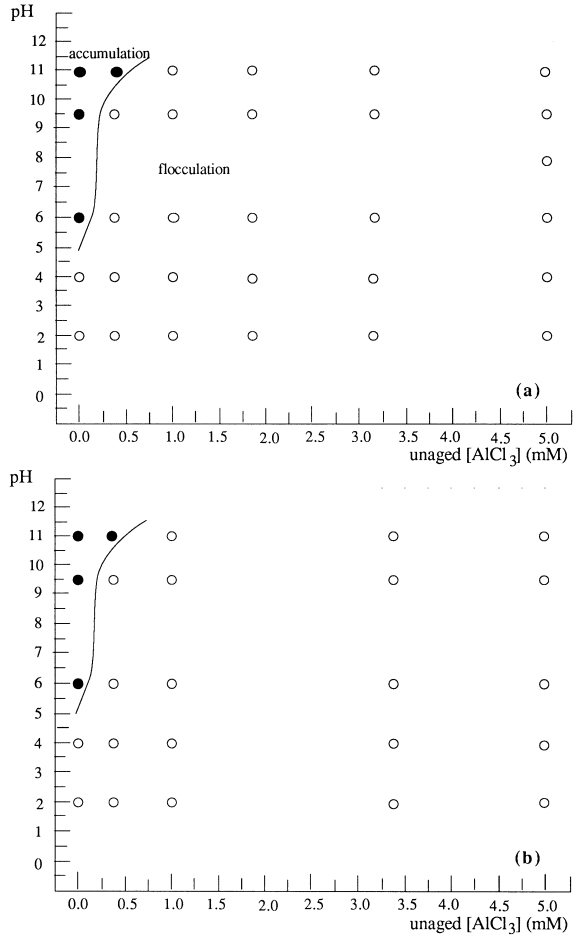

Fig. 5. Compared sedimentation diagrams of 1% montmorillonite suspensions mixed with unaged $AlCl_3$: (a) experimental observations; the solid and open dots respectively indicate accumulation and flocculation behavior; (b) diagram from the zeta potential data.The solid and open dots respectively indicate zeta potential absolute values $|\zeta| \geq 22$ mV and $|\zeta| \leq 22$ mV.

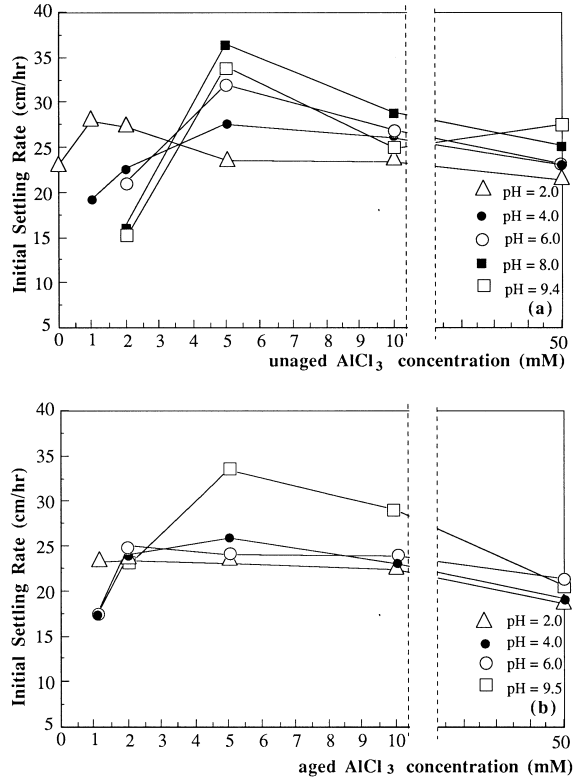

Fig. 6. Initial settling rate of 0·5% HUF Na-Kaolinite suspensions treated with $Na_4P_2O_7$, as a function of $AlCl_3$ concentration, at different pH: (a) unaged $AlCl_3$; (b) aged $AlCl_3$.

SEM micrographs which illustrate flocculated sediments obtained from mixed clay-unaged $AlCl_3$ suspensions are presented in Fig. 12 for kaolinite, and Fig. 13 for montmorillonite. These pictures show flocs which can be qualitatively described by the fractal DLA model. They also show that montmorillonite particles were extensively curled and they were much more thin than the kaolinite particles.

4 Discussion

In conditions where the present clay suspensions were prepared, kaolinite particles are known to carry negative charges both on their edges and faces.[2] The faces of montmorillonite particles are known to be negatively charged and the charge on their edges is controversial. However, these edges are much more thin than for kaolinite particles.

In these conditions, a first significant result of the present study was to illustrate the long range architecture of clay flocs formed in some sedimentation experiments. This architecture was actually very similar to the texture reported for clay-Fe flocs. In both cases, the micrographs were qualitatively consistent with fractal structures of the type predicted by Diffusion Limited Aggregation (DLA) models. By 'qualitatively', we mean that no fractal dimension f could practically be determined fom SEM micrographs. However, the micrographs characteristics were similar to the computer simulation characteristics reported for DLA aggregates.[5]

In terms of edge-to-face versus edge-to-edge particle association, the SEM micrographs tended to show that the association mode was driven by statistics. By this, we mean that quasi-edge-to-edge packing was frequently observed in flocculated sediments. That is to say linkage was between the edge of a first particle on one hand, and the face of a second particle but very close from the edge of this second particle on the other hand. Such a result was a priori consistent with the electrostatic theory applied to platelike particles, because the electrostatic repulsion energy decreases when the association mode progressively changes from true edge-to-face (i.e. in the middle of a face) to quasi-edge-to-edge, then to true edge-to-edge.[6] This statistical aspect is also enhanced by the fact that clay particles are not rectangular figures, but more or less distorted platelets with edges rather cut in random directions. Moreover, according to the electrostatic theory, the probability of quasi-edge-to-edge association should increase as platelike particles are thinner. This is consistent with the present data which showed that flocculation

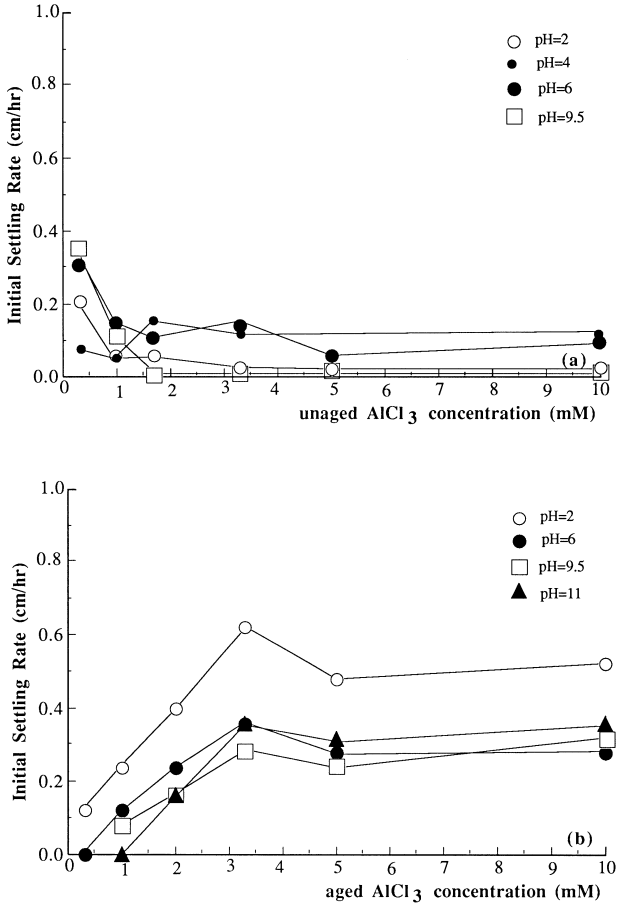

Fig. 7. Initial settling rate of 1% Na-montmorillonite suspensions as a function of $AlCl_3$ concentration and pH: (a) unaged $AlCl_3$; (b) aged $AlCl_3$.

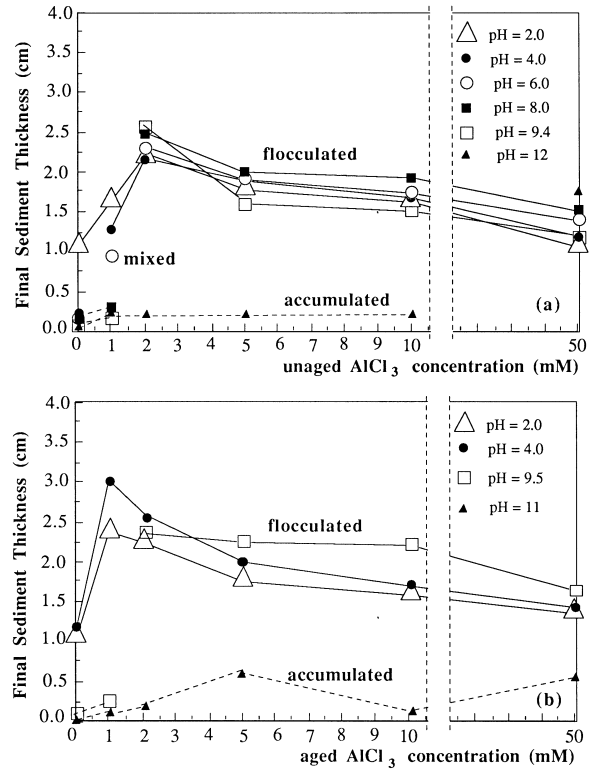

Fig. 8. Final sediment volume of 0·5% HUF Na-Kaolinite suspensions treated with $Na_4P_2O_7$, as a function of $AlCl_3$ concentration, at different pH. : (a) unaged $AlCl_3$; (b) aged $AlCl_3$.

occurred in a larger set of conditions with montmorillonite then with kaolinite.

This in turns introduces the second significant result of the present study, which showed that the type of clay aggregate architecture (i.e. open flocs, versus uniformly accumulated sediment) could be correlated with the absolute magnitude $|\zeta|$ of the zeta potential. That is to say, this correlation applied to all zeta potentials ζ with negative or positive values in Figs 10 and 11. Hence it appeared that the aggregation of clay particles, and also the sedimentation mode, were driven by electrostatic interactions. In the present case, the electrostatic theory on coagulation derived by Derjaguin, Landau, Verwey and Overbeek (DLVO theory)[7] could not be quantitatively applied in a straightforward fashion to calculate the interaction between particles. This is due to the fact that: (1) the counterions were Al^{3+} hydrolysis species and their nature, concentration and charge were not exactly known as they changed with time during the first hour after dissolution; (2) these hydrolysis species not only acted as counterions, but also as potential determining ions adsorbed on clay particles; (3) the clay particles were only colloidal in their thickness, not in their plate extent.

The mechanism by which Al electrolyte solutions help to link clay particles by the intermediate of Al gels to make relatively strong flocs, is known[8] and is consistent with our results. Electrolytes containing Al^{3+} undertake solvatation, hydrolysis and polymerization reactions,[9,10] when they are dissolved in aqueous medium. Actually, the only small species which is known to be really detected in solution is the trimer $[Al_3O_4(OH)_{24}(OH_2)_{10}]^{5+}$. Such trimers rapidly condense with a monomer to form the species $[Al_{13}O_4(OH)_{24}(OH_2)_{12}]^{7+}$ Which contains 13 Al atoms.[9] When a base is added to such solutions below 80°C, the accepted mechanism involves the formation of hexameric units. When an acid is added, trimers, tetramers and hexamers are formed. The solid which can be precipitated is the trihydroxide $Al(OH)_3$, as the bayerite or the gibbsite forms.[9]

These hydrolysis products from the Al^{3+} cations constitute counterions with respect to negatively charged clay particles. They also are potential determining ions for these clays, as they can exchange for Na^+.[11] The smaller Al oligomer species are fast reacting and they are more abundant in acidic conditions and in unaged than in aged Al^{3+} solutions. The hexameric planar species are rather present in aged solutions. They react more

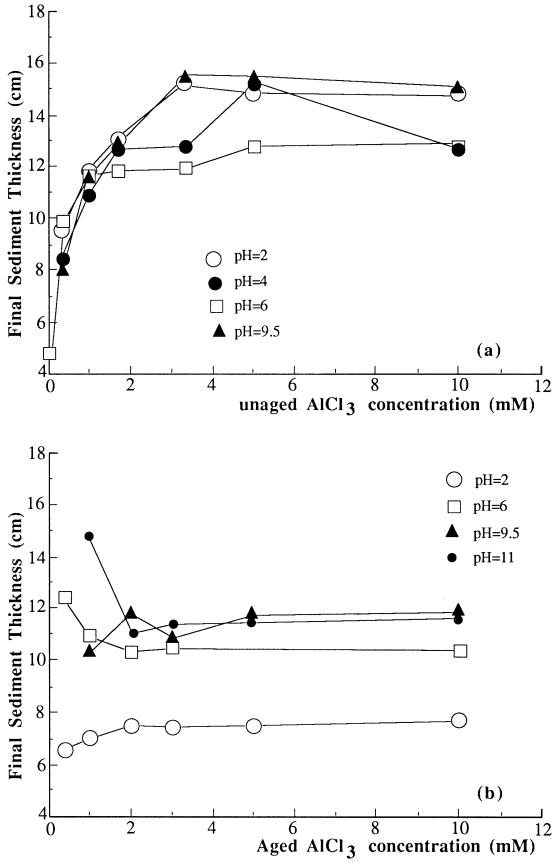

Fig. 9. Final sediment thickness of 1% Na-montmorillonite suspensions as a function of $AlCl_3$ concentration and pH: (a) unaged $AlCl_3$; (b) aged $AlCl_3$.

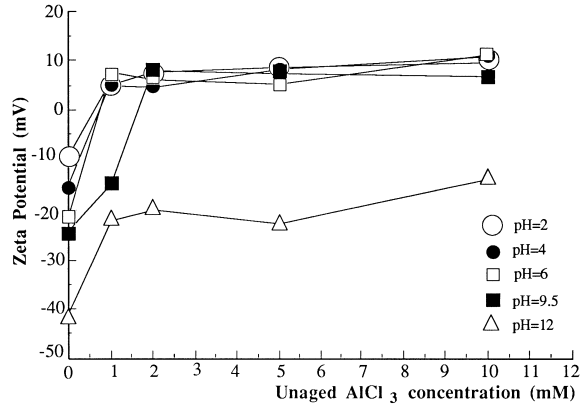

Fig. 10. Variation of the zeta potential with the concentration of unaged $AlCl_3$ at different pH values of kaolinite particles treated with $Na_4P_2O_7$.

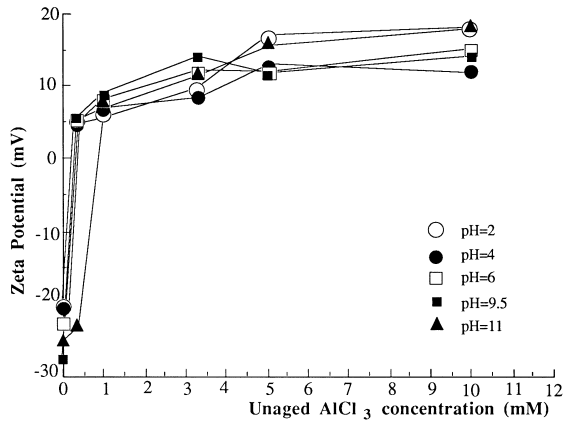

Fig. 11. Zeta potential of montmorillonite particles as a function of the concentration of unaged $AlCl_3$ in the suspension, at different pH.

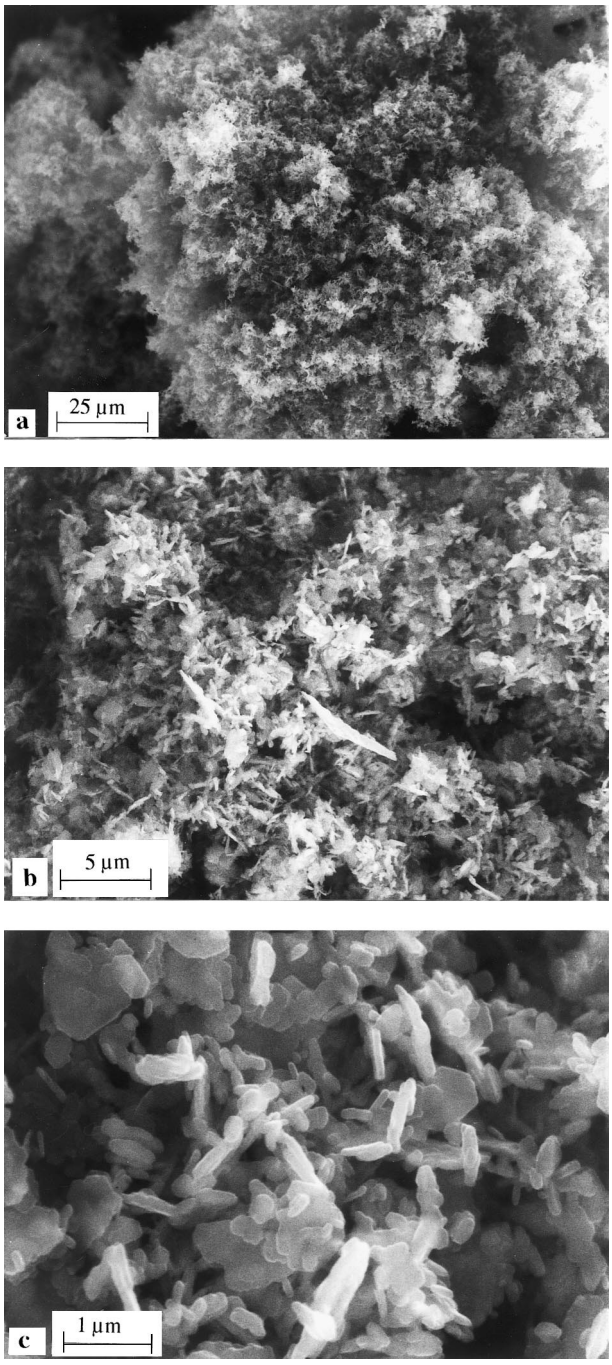

Fig. 12. SEM micrographs made at 15 kV and at several magnifications, of the flocculated sediment made from 0·5% kaolinite suspensions at pH 6 with an $AlCl_3$ concentration of: (a) 50 mM; (b) and (c) 2 mM.

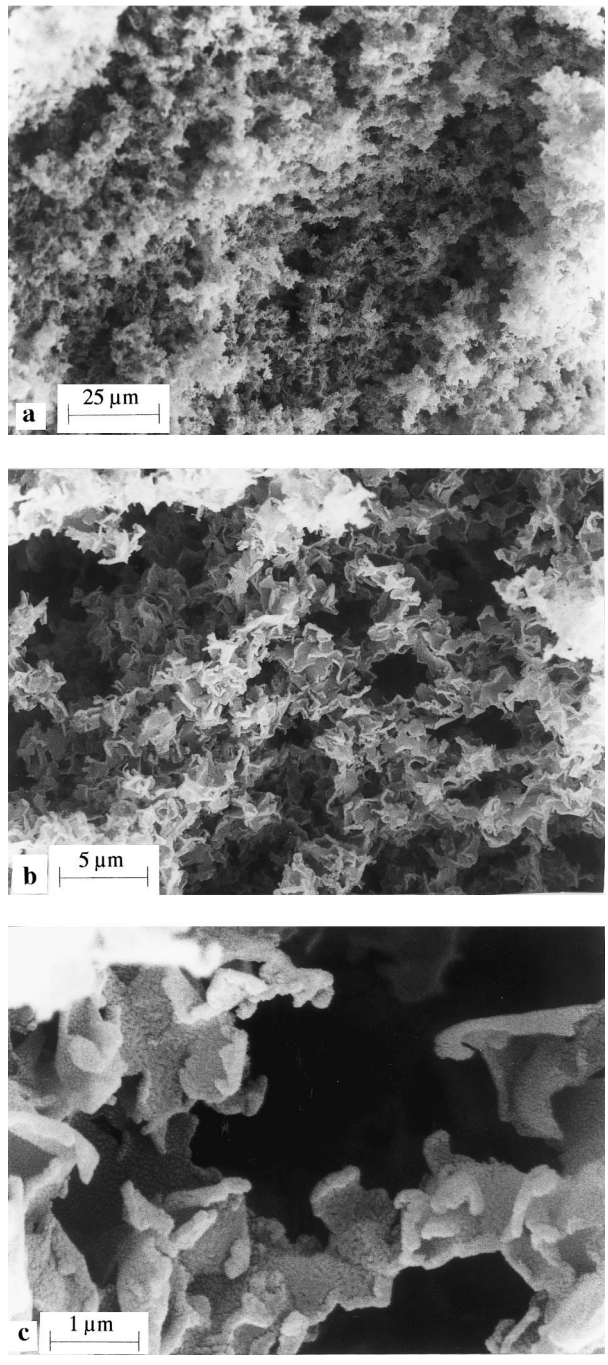

Fig. 13. SEM micrographs made at 15 kV and at several magnifications, of the flocculated sediment made from 1% montmorillonite suspensions at pH 9·5 with an $AlCl_3$ concentration of 2 mM.

slowly but they are better adsorbed because of their shape and their high charge.[12,13] At low Al concentration, these hexameric species can intercalate in between the layers of montmorillonite to which they can give a high specific area.[12,14] This is due to the fact that montmorillonite particles swell extensively in aqueous medium, while this phenomenon is very limited with kaolinite particles. Hence, it is not surprising that no significant difference was found between unaged and aged Al electrolyte, at low Al concentration, in the case of kaolinite, while a significant difference was found in the case of montmorillonite. On the other hand, at high Al concentration, these hexameric Al species provide an abundant coating on the faces of both kaolinite and montmorillonite particles, which explains that no big difference was found between aged and unaged Al electrolytes, with both types of clay.

5 Conclusion

The long-range architecture of kaolinite and montmorillonite flocs made with Al electrolytes is consistent with a combination of the electrostatic theory and the DLA theory. The first theory provides a

basis to explain the short range structure of aggregates. That is to say the linkage of two clay particles depends on their zeta potential, hence on their electrostatic repulsion. Also, the probability of particle association increases when the contact zone between two particles is closer from edge-to-edge. Critical values of the absolute magnitude $|\zeta|$ of the zeta potential: 12 mV for kaolinite and 22 mV for montmorillonie, discriminate between aggregation and flocculation mechanisms, which operate at zeta potential absolute magnitude respectively below and above the critical values. The second theory explains the long-range architecture of flocs (i.e. DLA fractal type aggregates), in terms of transport of particles.

Acknowledgements

This work was funded on a grant from NSERC, in Canada, which we are pleased to acknowledge.

References

1. Schofield, R. K. and Samson, H. R., *Disc. Farad. Soc.*, 1954, **18**, 135.
2. Swartzen-Allen, A. and Matijevic, E., *Chem. Rev*, 1974, **74**, 385.
3. Pierre, A. C., Zou, J. and Barker, C., *J. of Mat. Science.*, 1993, **28**, 5193.
4. Pierre, A. C., Ma, K. and Barker, C., *J. of Mat. Science.*, 1995, **30**, 2176.
5. Meakin, P., *Phys. Rev. A*, 1983, **27**, 604.
6. Pierre, A., *J. Can. Ceram. Soc.*, 1992, **61**, 135.
7. van Olphen, H., In Chemistry of Clays and Clay Minerals, ed. A. C. D. Newman. Longman Scientific and Technical Mineralogical Society, 1987, pp. 203–224.
8. Greenland, D. J., *Clay Miner.*, 1975, **10**, 407.
9. Henry, M., Jolivet, J. P. and Livage, J., *Structure and Bonding*, 1990, **25**, 259.
10. Livage, J., Henry, M. and Sanchez, C. *Prog. Solid State Chem.*, 1988, **18**, 259.
11. Hunter, R. J., *Foundations of Colloid Science*. Academic Press, San Diego, CA, 1982.
12. Oades, J. M., *Clays and Clay Min.*, 1984, **32**, 49.
13. Hsu, P. H., *Clays and Clay Min.*, 1992, **40**, 300.
14. Rengasamy, P. and Oades, J. M., *Aust. J. Soil. Res.*, 1978, **16**, 1978.